Exfoliated YBCO filaments for second-generation superconducting cable

2017 Supercond. Sci. Technol. 30 014006

(http://iopscience.iop.org/0953-2048/30/1/014006)

IOP Publishing Superconductor Science and Technology
Supercond. Sci. Technol. 30 (2017) 014006 (9pp) doi:10.1088/0953-2048/30/1/014006

Exfoliated YBCO filaments for second-generation superconducting cable

Vyacheslav Solovyov and Paul Farrell

Brookhaven Technology Group Inc., Advanced Energy Research and Technology Center, 1000 Innovation Road, Stony Brook, NY 11794, USA

E-mail: slowa@brookhaventech.com

Received 27 June 2016, revised 5 September 2016
Accepted for publication 21 September 2016
Published 15 November 2016

Abstract

The second-generation high temperature superconductor (2G HTS) wire is the most promising conductor for high-field magnets such as accelerator dipoles and compact fusion devices. The key element of the wire is a thin $Y_1Ba_2Cu_3O_7$ (YBCO) layer deposited on a flexible metal substrate. The substrate, which becomes incorporated in the 2G conductor, reduces the electrical and mechanical performance of the wire. This is a process that exfoliates the YBCO layer from the substrate while retaining the critical current density of the superconductor. Ten-centimeter long coupons of exfoliated YBCO layers were manufactured, and detailed structural, electrical, and mechanical characterization were reported. After exfoliation, the YBCO layer was supported by a 75 μm thick stainless steel foil, which makes for a compact, mechanically stronger, and inexpensive conductor. The critical current density of the filaments was measured at both 77 K and 4.2 K. The exfoliated YBCO retained 90% of the original critical current. Similarly, tests in an external magnetic field at 4.2 K confirmed that the pinning strength of the YBCO layer was also retained following exfoliation.

Keywords: coated conductors, exfoliation, cable

(Some figures may appear in colour only in the online journal)

1. Introduction

The core 2G wire technology can be described as a thin, <2 μm, $Y_1Ba_2Cu_3O_7$ (YBCO) layer deposited on a 50–100 μm thick metal substrate. To protect the substrate from oxidation, a 30–40 nm oxide stack is deposited on the metal substrate. Figure 1(a) shows the sequence of epitaxial layers in a rolling-assisted bi-axially textured substrate (RABiTS)-based 2G wire made by American Superconductor Corporation (AMSC) and figure 1(b) presents the actual cross-section of the AMSC 344 conductor. The 2G superconductors currently on the market are delivered as high aspect ratio tapes with a width of 4–12 mm and thickness of 100–150 μm [1, 2].

The existing 2G wire geometry has several drawbacks. First, the interfaces between ceramic layers are the weak mechanical links of the stack. For example, Barth *et al* [3] conducted extensive mechanical tests of 2G wire from the leading conductor manufacturers. They found that conductor failure typically occurs via delamination of the buffer-YBCO interface.

Second, 2G wire currently on the market is delivered as high aspect ratio tape with the wide side in the range of 4 to 12 mm. A high aspect ratio, such as $\approx$1:1000, causes high magnetization (AC) losses [4], which can be as high as tens of J/m for a high field magnet. This limits commercial application of the wire to low-field 77 K devices, such as transmission cables, fault-current limiters or large trapped-field synchronous motors and generators. A solution that would reduce AC loss is filamentization and transposition of the wire filaments. Currently, 2G wire filaments on the order of 0.5 to 1 mm have been demonstrated in lab scale (1 to 2 m coupons) [5, 6] and no transposition technology has yet been developed. It is also unclear whether such a wire can be practically jointed without shorting the filaments and thus negating the filamentization benefit.

Lastly, the superconducting layer is insufficiently stabilized because only the top stabilizer layer is in good electrical contact with the superconductor. The bottom (substrate) side of the superconductor is in contact with $\approx$30 nm of the insulating oxide buffer layer. To electrically connect the top and the

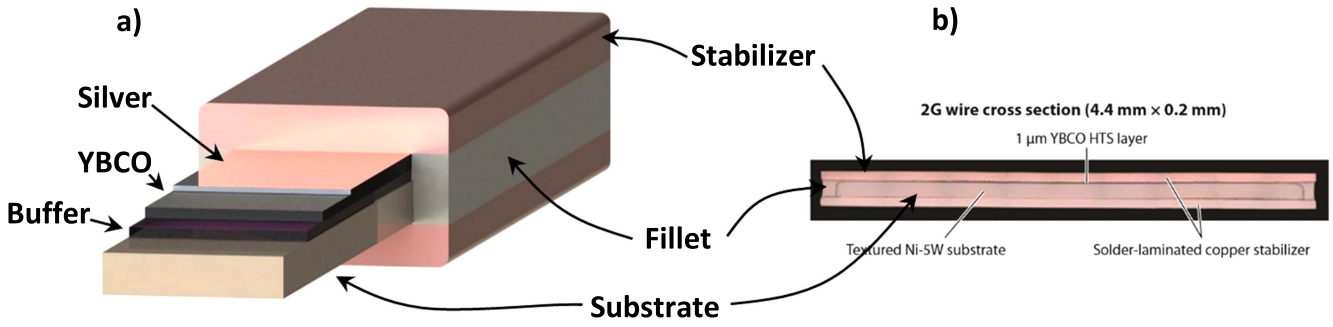

Figure 1. (a) Sequence of epitaxial layers in a typical 2 G wire. (b) Optical micrograph of a cross-section of 344 AMSC wire showing the actual ratio between thicknesses of the layers.

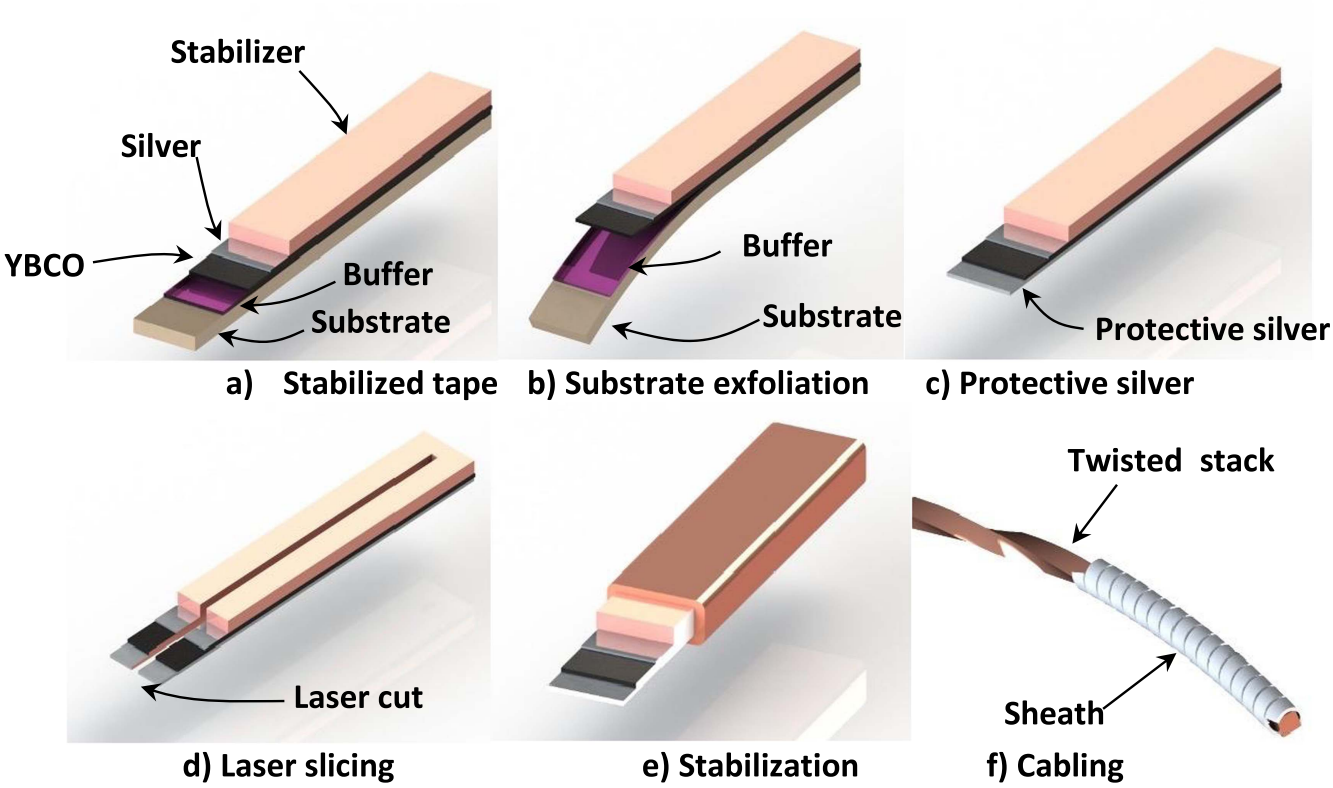

Figure 2. Steps of exfoliation.

bottom stabilizer layers a solder fillet is sometimes added at the conductor edges (see figure 1(a)). The fillet further reduces the superconductor fill factor, especially for narrow filaments.

Here, we show that a YBCO filament can be manufactured by mechanically separating the YBCO layer from the substrate by exfoliation. The exfoliated YBCO layers can be rapidly sliced by an industrial laser into narrow, 1 mm wide filaments, which can be further bundled into a cable. Elimination of the problematic YBCO-buffer interface, which is the weak point of the 2G wire architecture, improves both electrical and mechanical properties of the conductor.

2. Experiment

Figure 2 shows the four major steps of the process: (b) exfoliation of the substrate, (c) deposition of the protective silver layer, (d) laser slicing of the filament, and (e) plating of the filament with a stabilizing metal. Filaments can be bundled in a multi-stack cable as shown in panel (f). Each step is briefly described in the following.

Exfoliation experiments used AMSC standard wire (8602-FCL) as the starting material. The original wire is a 10 mm wide YBCO-RABiTS tape soldered between two 12 mm wide layers of 75 μm thick 316 L stainless steel foil by a low-temperature solder. The YBCO filaments were exfoliated after mechanically trimming the side fillets of the tape. To facilitate YBCO layer delamination, the tape was rapidly heated by an inductive coil coupled to the tape. The inductive coil was comprised of eight turns of gauge 14 multi-filament (Litz) wire wound to a 16 cm long and 1 cm wide racetrack shape. The high-frequency generator was designated as an H-bridge driven by optically isolated gate drives. External capacitors were used to form a resonant circuit. A series-

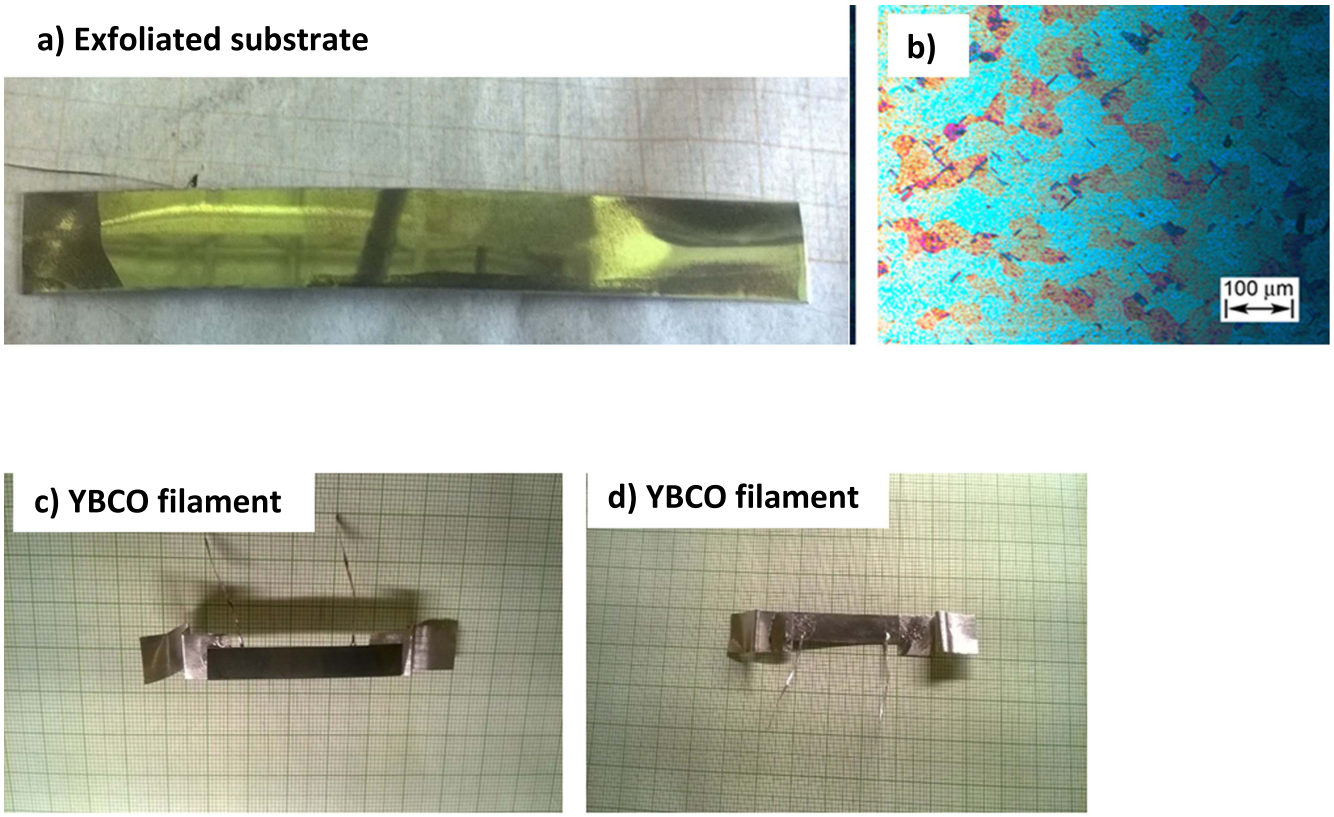

Figure 3. (a) Exfoliated substrate; (b) Optical micrograph of the substrate surface, demonstrating no residual YBCO; (c), (d) Exfoliated YBCO filament, supported by the stainless steel stabilizer, with current and voltage leads attached.

connected impedance was employed to match the impedance of the generator to the resonant circuit. Then, the coil was placed directly under the tape. This inductive coil design allowed for complete coupling of the AC field to the tape.

The coil was energized for 1 to 2 s by applying approximately 200 W of AC power at 50 KHz. An infrared thermometer monitored tape temperature during exfoliation. The YBCO layer was immediately exfoliated from the substrate. Typically, 10 cm long coupons were exfoliated in a single run. Figure 3(a) shows the exfoliated Ni substrate. Figure 3(b) presents an optical micrograph of the substrate surface. The micrograph demonstrates that complete exfoliation of YBCO was achieved with no residual YBCO left on the substrate. The exfoliated YBCO surface was studied via scanning electron microscopy using a Hitachi 480 scanning electron microscope (SEM) in the secondary electron mode.

After exfoliation, the YBCO layer is supported by the original top-side 75 um thick 316 L stainless steel foil, which serves as a stabilizer. To provide an electrical contact with the exfoliated surface, a 1 μm thick silver layer was deposited by magnetron sputtering. A 50 μm thick copper foil was soldered to the silver surface to provide additional protection of the YBCO layer. The current and voltage contacts can be easily attached to the stabilizer with a low-temperature solder, as shown in figures 3(c) and (d). Unless otherwise stated, the critical current density was measured by the DC transport method using 1 μV cm^{-1} electric field strength.

Tensile strength tests were performed at the Northrop Grumman Aerospace test facility, in Bethpage, New York, using an Instron series DX test machine. For testing purposes, 6 cm long and 1 cm wide exfoliated YBCO coupons were used. These coupons were clamped on each side so that an approximately 20 mm long segment could be used for transport measurements. To record a stress-strain calibration curve first, a film strain gauge was attached to the tape surface. The test coupon was stressed up to the failure point, which occurred at 620 MPa tensile stress. Afterwards, the stress–strain curve was used to estimate the strain level without attaching the strain gauge to each sample. Three coupons were strained below 0.6%, which is a typical critical strain level for YBCO layers [7, 8]. Two samples were strained at 0.6% and 0.8% to establish the failure mechanism. After stressing, the transport critical current, I_c, of the filament, was measured at 77 K self-field. Afterwards, bending tolerance was tested by wrapping the filaments around a mandrel and measuring I_c at 77 K.

The exfoliated YBCO coupons were sliced into 1, 2, and 4 mm strips by a low-wattage ($<$100 W) CO_2 laser. Laser slicing was performed by Kern Laser Systems LLC, Wadena, Minnesota. The samples were patterned by moving the optical table. No active cooling of the tape was provided during laser slicing.

To perform 4.2 K in-field transport measurements, a 1 mm wide filament sample was mounted on a specially made G10 holder with GE varnish. An 8 T Nb-Ti superconducting

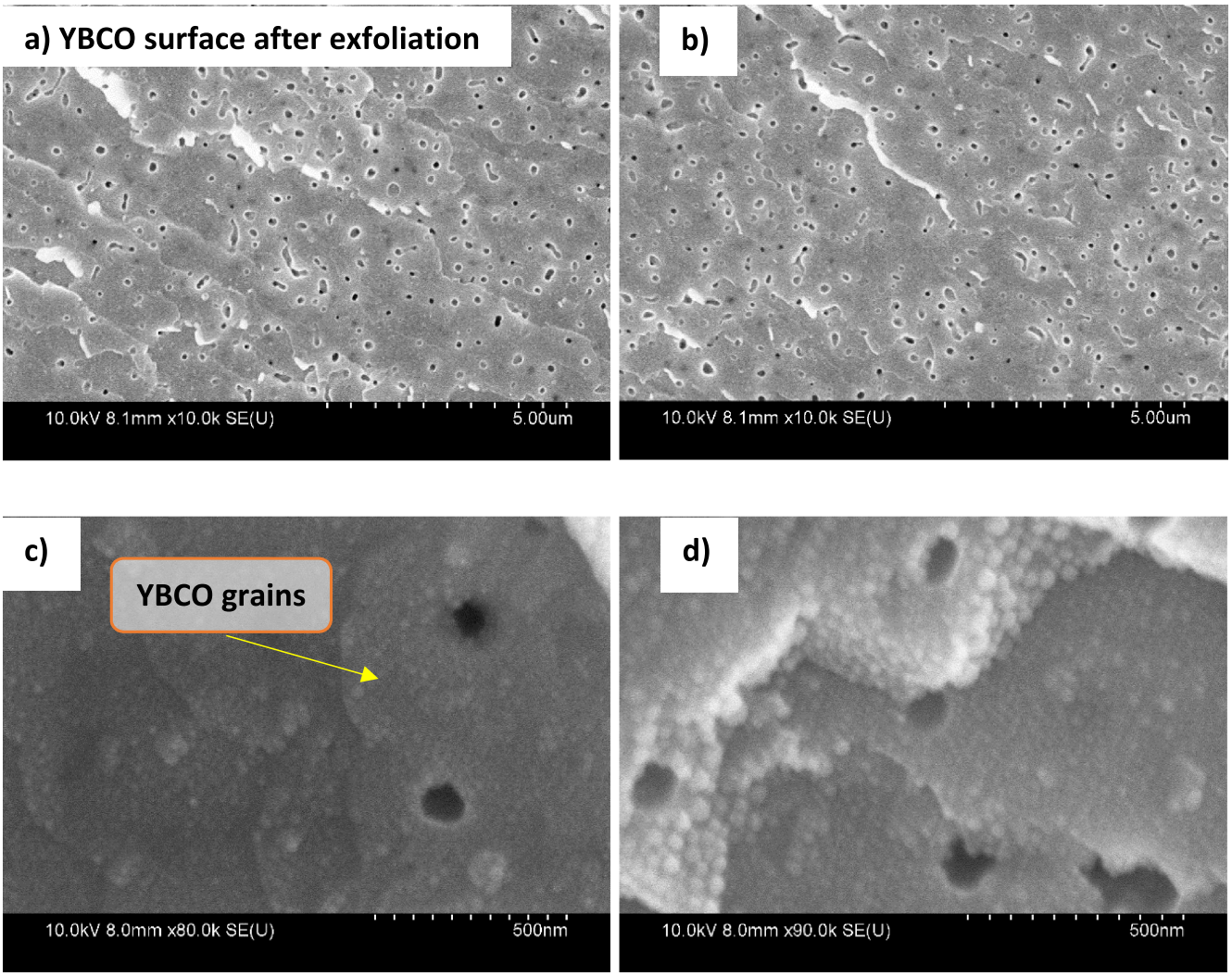

Figure 4. SEM plan views of the exfoliated YBCO surface. (a), (b) Low resolution SEM images; (c), (d) high resolution SEM images.

magnet generated the background magnetic field. The *I*–*V* curves were recorded in DC 4-point mode; the maximum current was 300 A.

3. Results and discussion

3.1. Electrical and structural characterization

Figure 4 shows a series of SEM plan views of the exfoliated YBCO surface. The surface morphology contains characteristic pores that are typically found in YBCO layers produced by the metal organic deposition (MOD) method, such as that used by AMSC to grow the YBCO layers. The circular features in figures 4(c)–(d), 0.5 μm in diameter, are most likely YBCO grains that originate from a nucleation point in the center circle.

To estimate the height of the terraces visible in figure 4, measurement was repeated in the edge view mode (see figure 5). The sample was tilted at 70° with respect to the electron beam. These SEM micrographs provide an estimation of the terrace height, which is 50 ± 20 nm on average. These measurements confirm that most of the YBCO layer is removed from the substrate intact. Indeed, the original YBCO film thickness is 1.2 μm; however, the 50 nm height variation of the exfoliated YBCO surface indicates that loss of YBCO due to exfoliation is less than 5%. This is further confirmed by comparing the critical current density, J_c, of the exfoliated filaments with the critical current density of the original tape.

Figure 6(a) shows optical micrographs of the exfoliated YBCO coupons after being sliced by the 100 W Kern CO_2 laser into 0.8 mm filaments. Figure 6(b) is a detailed view of the cut. The cut is approximately 50 μm wide with some minor damage visible at the edges.

Figure 7(a) shows examples of *I*–*V* curves of 0.8 mm and 1.8 mm wide exfoliated YBCO filaments sliced with the CO_2 laser. Here the horizontal dashed line indicates the 1 μV cm^{-1} electric field strength level that was used to determine the critical current density. Figure 7(b) summarizes the dependence of the critical current density on the filament width. The dashed area represents the I_c ranges of the original tape, 260 ± 10 A cm^{-1}. Figure 7(b) proves that exfoliation and laser slicing do not appreciably damage the superconducting layer.

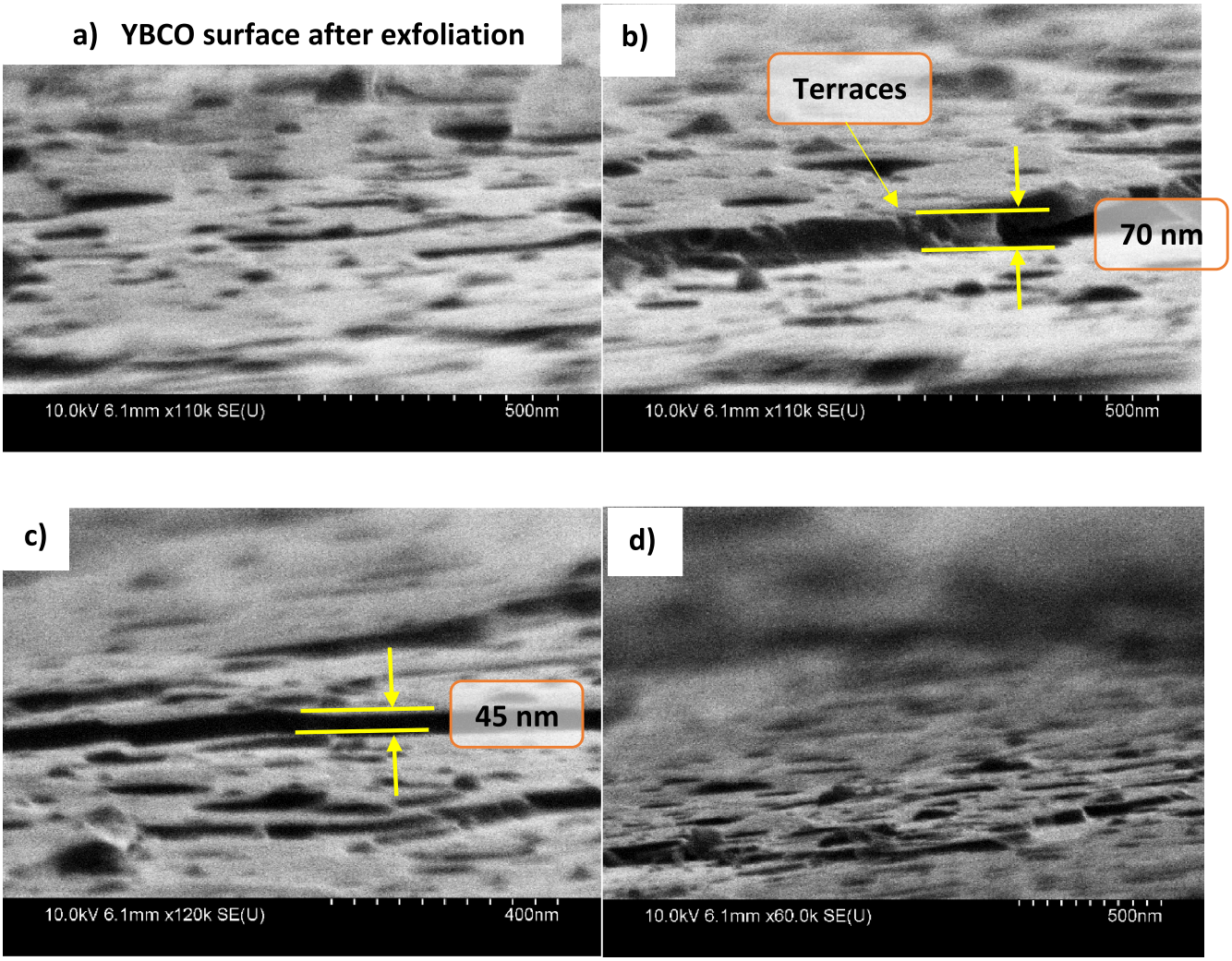

Figure 5. High-resolution SEM images of the exfoliated YBCO surface, edge view. The arrows in panels (b)–(c) show the height of the YBCO layer terraces.

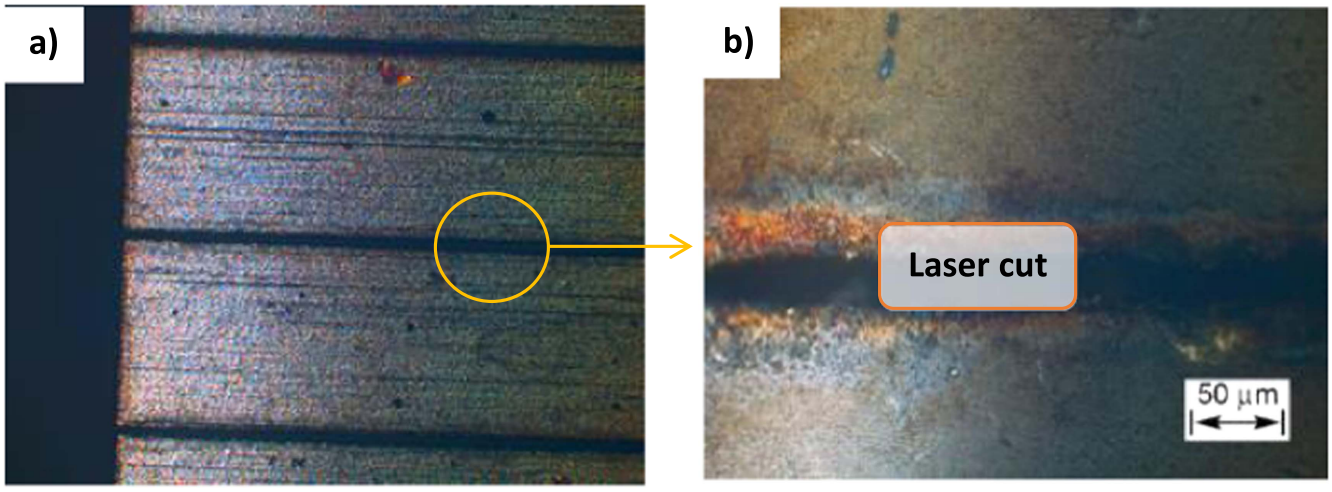

Figure 6. Optical micrographs of the exfoliated YBCO coupons after slicing. (a) The 0.8 mm wide filament cut with the CO_2 laser; b) Detailed view of the filament cut; the cut width is approximately 50 μm. Both panels show the YBCO side of the filament.

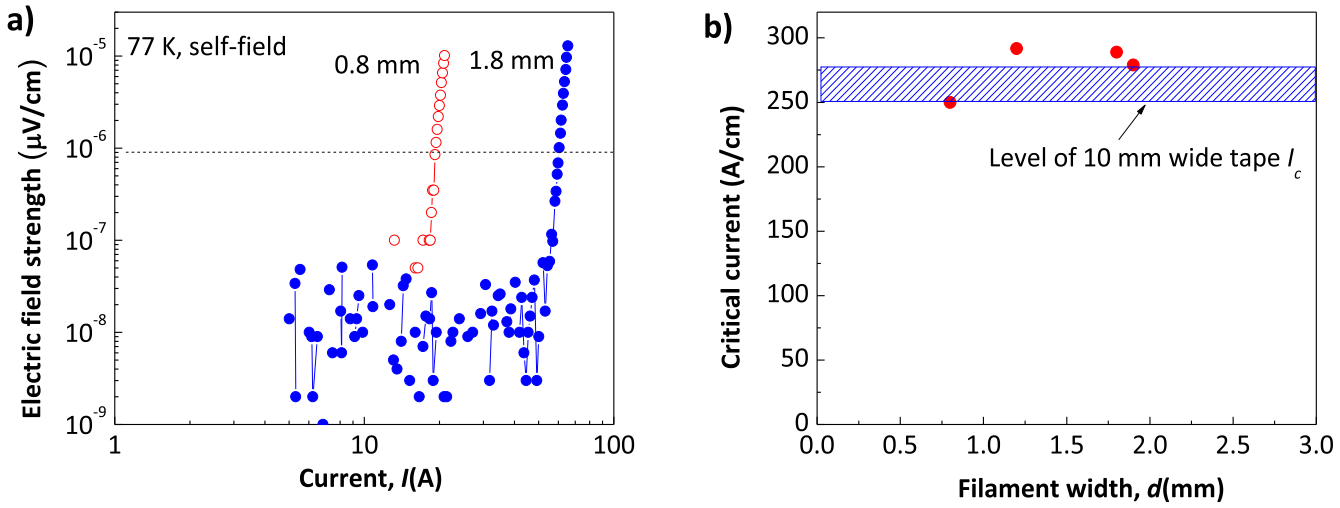

Figure 7. (a) 77 K *I–V* curves of 0.8 mm and 1.8 mm wide filaments; (b) Dependence of the critical current density of the filaments on filament width; the dashed area represents the ranges of the original I_c of the tape.

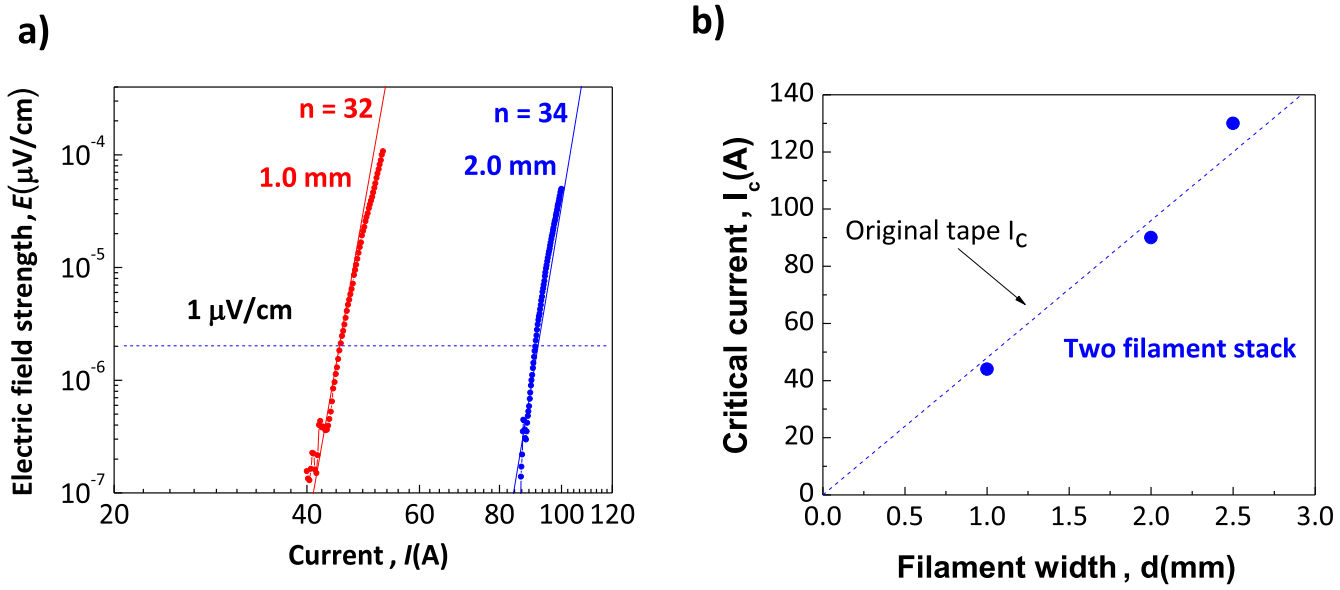

Figure 8. (a) *I–V* curves of 1.0 and 2.0 mm wide exfoliated two-filament stacks. The solid lines are the power law best-fit approximations. (b) Critical current densities of 1 and 2 mm two-ply wire coupons. The dashed line represents the I_c level of the original tape.

Figure 8(a) compares 77 K *I–V* curves of untwisted two-filament stacks. The sample length is 10 cm. The I_c of the double-filament stack is twice that of a single filament, which is an indication of good electrical coupling between the filaments. The *n*-values, obtained in the power law fit are 32 and 34 for 1 mm and 2 mm wide stacks, respectively. Note that these *n*-values are typical for the standard AMSC wire at 77 K [9]. Figure 8(b) plots the width dependence of the stack I_c. The dashed line is the projected I_c of a two-filament stack comprised of the original tape.

Figure 9(a) presents *I–V* curves of the 1 mm wide filament at 4.2 K for magnetic field values ranging from 0 to 5.3 T. The *n*-factor was determined to be in excess of 35 for fields up to 5.3 T, H||c. Figure 9(b) shows the critical current density as a function of the applied magnetic field at 4.2 K. The horizontal line shows the level of self-field I_c for the original tape sample. The dashed line in figure 9(b) is the power law approximation $I_c \sim 1/B^{\alpha}$. The α exponent value as determined from the best fit is 0.8 ± 0.05.

3.2. Mechanical tests of exfoliated filaments

Figure 10(b) shows a complete tensile stress–strain curve of the 10 mm wide exfoliated YBCO filament. The filament exhibited onset of yield at 500 MPa stress and failed at 560 MPa, which is well within the expected range of the 316 L steel used as the stabilizer. Five coupons were pre-stressed at 0.05, 0.12, 0.25, 0.6, and 0.8%. These levels are indicated in figure 10(b) (red stars). The solid symbols represent normalized (with respect to the unstrained state)

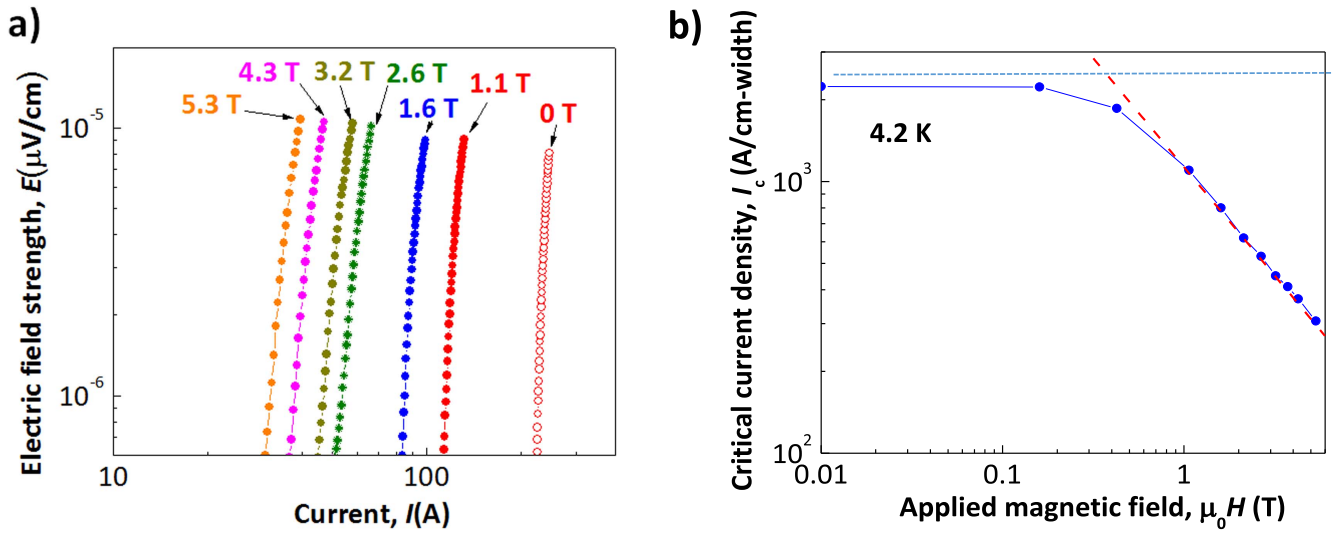

Figure 9. (a) *I–V* curves of the filament recorder at 4.2 K, up to 5.3 T; (b) The critical current density as a function of applied magnetic field, 4.2 K, H||c. The horizontal line indicates the self-field I_c level of the original tape (before exfoliation). The dashed line is the power law best-fit approximation.

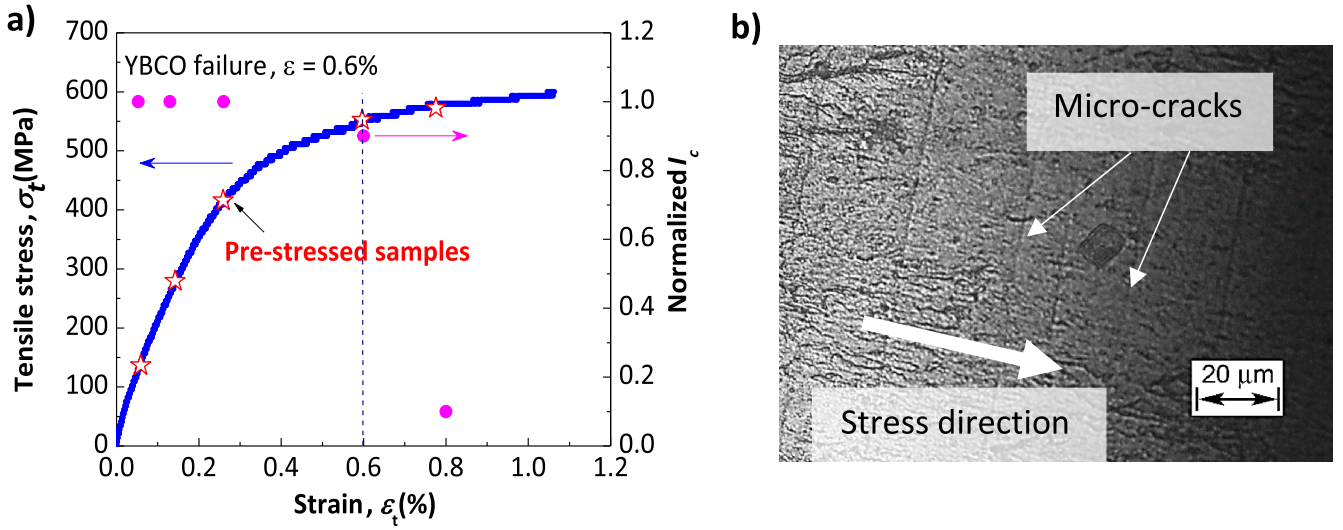

Figure 10. (a) Stress-strain curve of the filament. The red stars indicate the stress level of filaments used for the *ex situ* critical current measurements. The right axis presents the dependence of I_c on strain. (b) Optical micrograph of the surface of the YBCO filament stressed at 560 MPa. Cracks propagating perpendicular to the stress direction are well visible.

critical current density as a function of strain. The superconducting layer fails at a strain level >0.6%. Optical inspection of the sample strained at 0.8% reveals multiple micro-cracks running perpendicular to the direction of stress application. The micro-cracks are most likely responsible for the rapid degradation of I_c at the strain level >0.6%.

Bending test for a two-stack coupon are presented in figure 11(a)). The sample exhibits no critical current degradation after bending at >10 mm radius in both directions. The I_c value rapidly deteriorated after bending at a 5 mm radius. Figure 11(b) summarizes the results of the bending tests. The critical bending radius, defined by degradation of I_c below 90% of the original, is 15 mm for a two-stack sample and 10 mm for a single filament.

4. Discussion

Since the first 2G wire was manufactured in 1995 [10], the buffered metal substrate has been considered an indispensable part of a 2G wire. It was realized early on that the substrate must comply with sometimes conflicting requirements: on one hand, it should serve as a high temperature oxidation-resistant template for YBCO growth; on the other hand, it should provide mechanical support and conductor stabilization at cryogenic temperatures. Reconciling these requirements was especially challenging for RABiTS technology [11]. The original RABiTS substrate is a textured nickel foil. Pure nickel is rather soft and ferromagnetic; both qualities are undesirable for a superconducting wire. These problems were

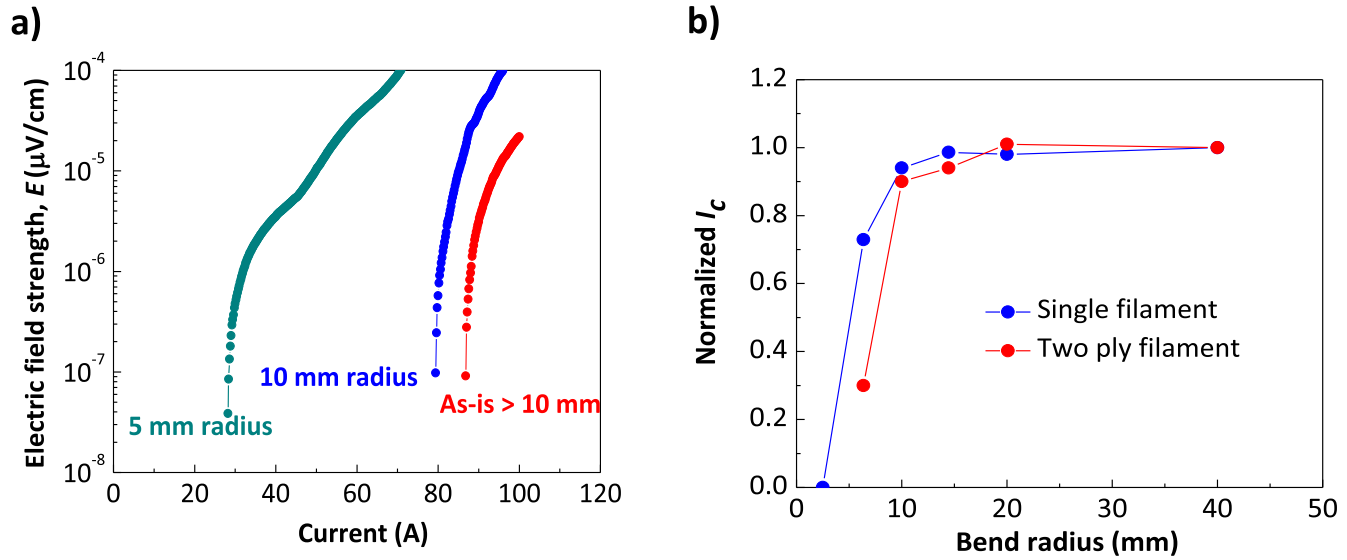

Figure 11. (a) *I–V* curves of a two-ply filament subjected to bending at 10 mm and 5 mm radius. The results of the bending *I–V* curve did not change appreciably for the bending radii >15 mm. (b) Dependence of the normalized critical current density of a single filament and a two-ply stack on the bending radius.

somewhat alleviated by using Ni-W alloys instead of pure Ni [12], however the more complex metallurgy of Ni-W added cost to the wire.

Exfoliation, which can be described as a process of separation of useful material layer from a bulk substrate, has long been a cornerstone of many industrial processes, for example, silicon-on-insulator technology [13]. To exfoliate silicon, a large amount of hydrogen is implanted into the substrate so that hydrogen bubbles are formed and hydrogen-induced cracking assists exfoliation. Here, it is shown that exfoliation of the YBCO-CeO_2 interface does not require this implantation assistance because YBCO is weakly attached to the substrate. It has been demonstrated that YBCO, especially in metal-organic deposition (MOD) processes, nucleates in very few locations of the substrate [14]. Indeed, YBCO grains seen in figures 4(c)–(d) are quite large, up to 0.5 μm. Such a grain structure is formed because YBCO has a highly anisotropic growth habit: it grows ten times faster in the *ab* plane than in the *c* direction. Thus, most of the substrate is covered by lateral overgrowth with little or no chemical bonding between the substrate and YBCO. This explains why the YBCO layer can be separated practically intact, as evidenced by the retention of the critical current density in exfoliated YBCO filaments (see figures 7–8) and the absence of low temperature pinning degradation (see figure 9).

The mechanical tests, figure 10, confirm that the tensile strength of the exfoliated filaments is limited by the strength of the stainless steel stabilizer, which is much higher than the strength of the Ni substrate. Failure of the superconducting layer occurs when the strain level exceeds 0.6%, which is in good agreement with the literature data [15, 16]. These experiments also demonstrate a practical pathway towards an ultra-high strength, low cost conductor. Since the stabilizer supporting the exfoliated YBCO layer is not required to have high temperature oxidation resistance, low cost high-carbon steels can be readily utilized as a mechanical support and stabilizer. For example, C1095 steel has tensile strength of 1379 MPa, far exceeding the 755 MPa of the water-quenched C-22 Hastelloy currently used in the IBAD process.

Finally, results of bending tests in figure 11 demonstrate high flexibility of the filaments. These bending tolerances of the filaments compare favorably with the typical 20 mm bending radius of a standard 2G wire [17] and 40 mm for stainless steel laminated DI-BSCCO tape [18] (manufactured by Sumitomo Electric Industries). Elimination of the substrate will possibly improve performance of a multi-strand cable. Multi-strand 2G wire cables [19, 20] under development for fusion and magnet applications suffer from poor current sharing between filaments due to the insulating buffer coating of the substrate. This complicates quench detection and protection of magnets wound using such cables: a normal zone in one of the filaments may remain undetected by a voltage tap method, thus necessitating development of alternative quench detection techniques. Exfoliated filaments would be electrically coupled, thus allowing use of traditional quench detection and protection methods.

5. Conclusion

In conclusion, it is feasible to reliably separate a YBCO layer from the substrate on a 10 cm scale. The exfoliated YBCO filament is supported by a stainless steel stabilizer, which is shown to have better mechanical properties than the substrate. This development enables the design of application-specific superconducting cables with electrical and mechanical properties that are not limited by the substrate. Future efforts will be focused on scaling up the process and demonstrating filament and cable performance on a tens of meter scale.

Acknowledgments

The work at Brookhaven Technology Group was supported by the Department of Energy, Office of High Energy Physics under Small Business Innovation Research (SBIR) Phase I award DE-SC0013856. The authors wish to thank Marty Rupich of American Superconductor Corporation for providing the 2G wire coupon, Robert Fidnarick of Northrop Grumman Corporation for performing the mechanical tests, and Thomas Buzek for helpful suggestions.

References

[1] Fleshler S, DeMoranville K, Gannon J Jr, Li X, Podtburg E, Rupich M W, Sathyamurthy S, Thieme C L H, Tucker D and Whitman L 2014 Development status of AMSC amperium (R) wire *11th European Conf. on Applied Superconductivity (Eucas2013)* vol 507 Pts 1-4

[2] Selvamanickam V *et al* 2011 Progress in performance improvement and new research areas for cost reduction of 2G HTS wires *IEEE Trans. Appl. Supercond.* **21** 3049–54

[3] Barth C, Mondonico G and Senatore C 2015 Electro-mechanical properties of REBCO coated conductors from various industrial manufacturers at 77 K, self-field and 4.2 K, 19 T *Supercond. Sci. Technol.* **28** 045011

[4] Wilson M N 1983 Superconducting magnets *Monographs on Cryogenics [2]* (Oxford Oxfordshire New York: Clarendon Press; Oxford University Press) xv p 335

[5] Kesgin I, Levin G A, Haugan T J and Selvamanickam V 2013 Multifilament, copper-stabilized superconductor tapes with low alternating current loss *Appl. Phys. Lett.* **103** 252603

[6] Suzuki K, Yoshizumi M, Izumi T, Shiohara Y, Iwakuma M, Ibi A, Miyata S and Yamada Y 2008 Development of scribing process of coated conductors for reduction of AC losses *Physica C: Superconductivity* **468** 1579–82

[7] Floegel-Delor U, Riedel T, Wippich D, Rothfeld R, Schirrmeister P, Koenig R, Werfel F N, Usoskin A and Rutt A 2014 Operation and experience of a 2 km coated conductor REEL—to—REEL copper pulse plating facility *J. Phys.: Conf. Ser.* **507** 022006

[8] Cheggour N, Ekin J W, Clickner C C, Verebelyi D T, Thieme C L H, Feenstra R and Goyal A 2003 Reversible axial-strain effect and extended strain limits in Y-Ba-Cu-O coatings on deformation-textured substrates *Appl. Phys. Lett.* **83** 4223–5

[9] Fleshler S, DeMoranville K, Gannon J Jr, Li X Jr, Podtburg E, Rupich M W, Sathyamurthy S, Thieme C L H, Tucker D and Whitman L 2014 Development status of AMSC amperium reg wire *J. Phys.: Conf. Ser.* **507** 022005–0022009

[10] Wu X D *et al* 1995 Properties of $YBa_2Cu_3O_7$-delta thick-films on flexible buffered metallic substrates *Appl. Phys. Lett.* **67** 2397–9

[11] Goyal A *et al* 1996 High critical current density superconducting tapes by epitaxial deposition of YBa2Cu3Ox thick films on biaxially textured metals *Appl. Phys. Lett.* **69** 1795–7

[12] Goyal A, Paranthaman M P and Schoop U 2004 The RABiTS approach: using rolling-assisted biaxially textured substrates for high-performance YBCO superconductors *MRS Bull.* **29** 552–61

[13] Bruel M 1996 Application of hydrogen ion beams to silicon on insulator material technology *Nucl. Instrum. Methods Phys. Res. B* **108** 313–9

[14] Solovyov V F, Develos-Bagarinao K, Li Q, Qing J and Zhou J 2010 Nature of $YBa_2Cu_3O_7$ nucleation centers on ceria buffers *Supercond. Sci. Technol.* **23** 014008

[15] Katagiri K, Tsunematsu Y, Ishikawa Y, Takahashi T, Kasaba K, Kuroda T and Itoh K 2008 Strain characteristics of critical current in RABiTS/Y-Ba-Cu-O coated conductors *Physica C: Superconductivity* **468** 1697–701

[16] Takao T *et al* 2007 Influence of bending and torsion strains on critical currents in YBCO coated conductors *IEEE Trans. Appl. Supercond.* **17** 3513–6

[17] Markiewicz W D and Swenson C A 2010 Winding strain analysis for YBCO coated conductors *Supercond. Sci. Technol.* **23** 045017

[18] Yamazaki K, Kagiyama T, Kikuchi M, Yamade S, Nakashima T, Kobayashi S, Osabe G, Fujikami J, Hayashi K and Sato K 2012 Recent progress on improvement to mechanical properties of DI-BSCCO wire *Supercond. Sci. Technol.* **25** 054015

[19] Uglietti D, Bykovsky N, Sedlak K, Stepanov B, Wesche R and Bruzzone P 2015 Test of 60 kA coated conductor cable prototypes for fusion magnets *Supercond. Sci. Technol.* **28** 124005

[20] Laan D.C.v.d., Goodrich L F, Noyes P, Trociewitz U P, Godeke A, Abraimov D, Francis A and Larbalestier D C 2015 Engineering current density in excess of 200 A mm −2 at 20 T in CORC ® magnet cables containing *Supercond. Sci. Technol.* **28** 124001